

Atmospheric Fate of Methyl Vinyl Ketone: Peroxy Radical Reactions with NO and HO₂

Supporting Information

Eric Prasket[†], John D. Crounse^{‡}, Kelvin H. Bates[†], Theo Kurtén[¶], Henrik G. Kjaergaard^{¶¶}, Paul*

O. Wennberg^{#§}

[†]Division of Chemistry and Chemical Engineering, California Institute of Technology, 1200 E.
California Blvd, Pasadena, California 91125, United States

[‡]Division of Geological and Planetary Sciences, California Institute of Technology, 1200 E.
California Blvd, Pasadena, California 91125, United States

[¶]Department of Chemistry, University of Helsinki, P.O. Box 55, Helsinki, 00014, Finland

^{¶¶}Department of Chemistry, University of Copenhagen, Universitetsparken 5, 2100 Copenhagen
Ø, Denmark

[§]Division of Engineering and Applied Science, California Institute of Technology, 1200 E.
California Blvd, Pasadena, California 91125, United States

*Email: crounjd@caltech.edu

INSTRUMENTAL CALIBRATION. CIMS sensitivity factors are determined by the specific molecule-ion collision rates and the binding energy of the resulting clusters. The rate of collision can be estimated from the dipole moment and polarizability of the analyte.¹ These properties were calculated using DFT for the C₄ compounds produced in the oxidation of MVK. Because the dipole moment depends on the structural conformation of the molecule, we calculate the population density and dipole of all conformers with a relative population of >5% at 298 K to estimate the conformationally-weighted property. The polarizability was not found to exhibit significant conformational dependence and the calculation was therefore based on the lowest energy structure. Further detail of similar calculations is provided by Garden et al.² A summary of these properties along with calibration factors for MVK systems is shown in Table S1.

Table S1. Calculated conformer-weighted dipole moments (μ) and polarizabilities (α) served as the basis for sensitivity determination (see Paulot et al.,³ unless otherwise noted). k_x is the weighted average of the calculated collision rates (see Su et al.¹) for conformers having an abundance greater than 5%. These are normalized to the average of the calculated collision rates for CF_3O^- with MVKN and MVKN' at 298 K ($k = 1.8 \times 10^{-9} \text{ cm}^3 \text{ molecule}^{-1} \text{ s}^{-1}$) and the mean of the experimentally determined MVKN and MVKN' sensitivities was used to infer the sensitivity for compounds for which no standards were available. Masses (m/z) represent the cluster mass with CF_3O^- . For compounds reacting with CF_3O^- to form multiple product ions, the sum of all known product ions have been used for quantification. Isoprene nitrate (1-hydroxy-3-methylbut-3-en-2-yl nitrate, ISOPN-4,3) has been included for additional comparison between theory and experiment.

molecule	m/z	μ (D)	α (\AA^3)	$k_x(10^{-9} \text{ cm}^3 \text{ molecule}^{-1} \text{ s}^{-1})$	calculated sensitivity ($\times 10^{-4}$) ^a	experimental sensitivity ($\times 10^{-4}$) ^a
ISOPN-4,3	232	2.5	11	1.9	3.1	3.7
glycolaldehyde	145	2.3	4.5	2.0	3.1	3.0 ± 0.2 ^b
hydroxy diketone	187	2.1 ^c	7.2 ^c	1.8	2.7	-
4,3-hydroxy-hydroperoxide	205+139 +101+63	2.6 ^c	8.1 ^c	2.0	3.1	-
MVKN	234	2.3	9.9	1.8	2.8	2.6 ± 0.3 ^b
MVKN'	234	2.2	9.7	1.8	2.7	3.0 ± 0.3 ^b

^a CF_3O^- CIMS sensitivity (norm. cts. pptv^{-1})

^b Hydroxy nitrate sensitivities were determined using thermal dissociation LED-induced fluorescence⁴ and glycolaldehyde was calibrated as described in the current work. Uncertainties are indicated for measured sensitivities.

^c Calculated in support of this work by HGK at the B3LYP/6-31G(d) level.

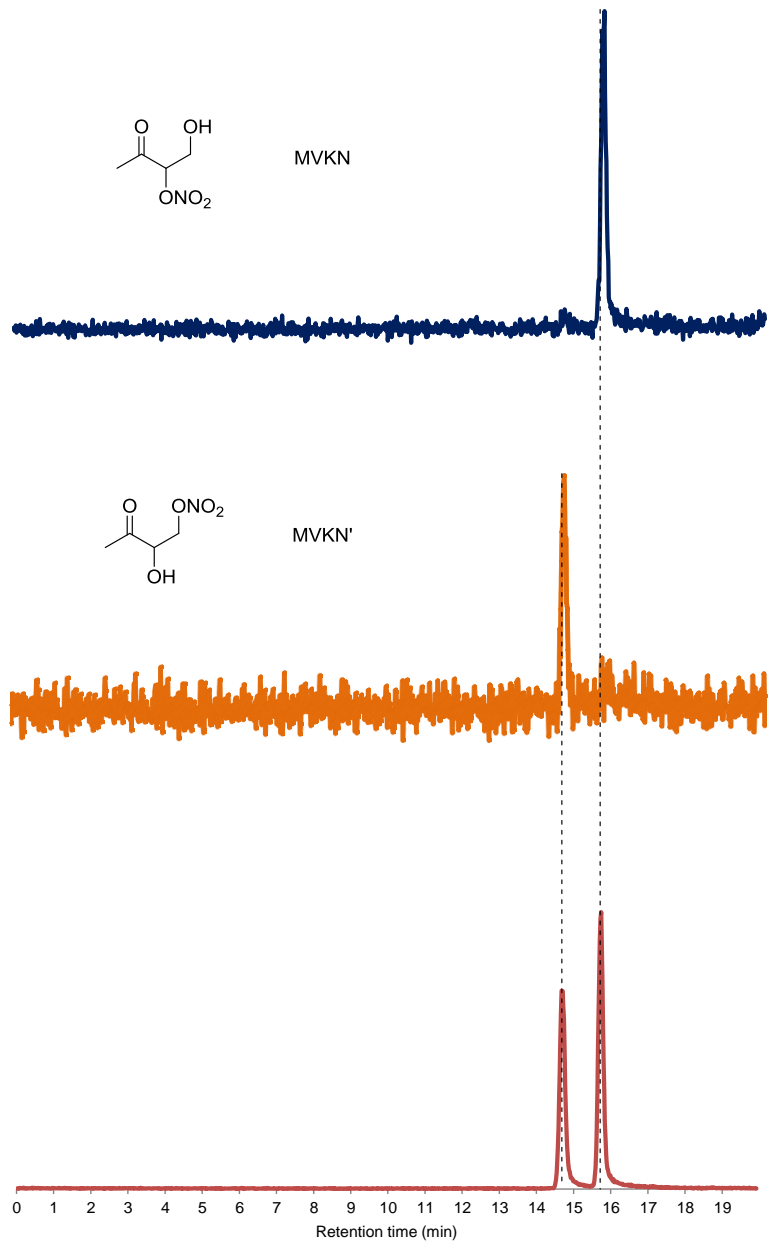


Figure S1. Chromatographic analysis used for the identification of MVKN and MVKN'. Data are derived from experiments 8 (bottom panel), 14 (mid panel), and 12 (top panel). The latter two experiments isolated the chemistry of individual RO₂, enabling the structures and retention times of the individual organic nitrates to be discerned. This assignment also matches the elution order previously reported using a similar column.⁵

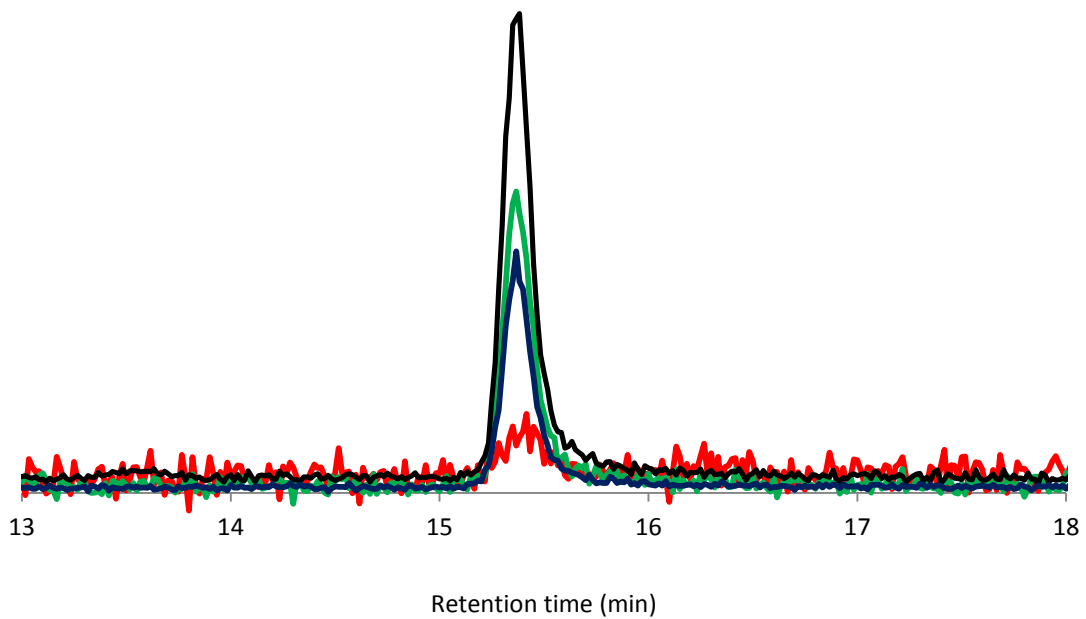


Figure S2. Chromatographic analysis of the 4,3 hydroxy hydroperoxide derived from experiment 1. Shown are the major product ions in order of descending area: m/z 139 (black), m/z 101 (green), m/z 205 (blue), m/z 63 (red).

CHEMICAL TRANSPORT MODEL. The following section describes changes made to the GEOS-Chem mechanism (Table S2 – Table S3).⁶ The maps (Figure S3 – Figure S5) illustrate the output of the model resulting from the changes. These simulations employ GEOS-Chem v9-02 using GEOS5 meteorology and initialize the model with a 1.5 year spinup before the January – December 2012 final simulation. The Rosenbrock Rodas-3 with Kinetic PreProcessing software was used as the solver.

Table S2. Revisions incorporated into the GEOS-Chem mechanism. The scenarios are consistent with those described by Table 5. The base scenario includes the alkyl nitrate branching determined in this work. Naming conventions used below can be found at <http://wiki.seas.harvard.edu/geos-chem>.

scenario	base model	revised model
Base ($\text{VRO}_2 + \text{NO} \rightarrow$)	$0.88\text{NO}_2 + 0.35\text{HO}_2 + 0.35\text{CH}_2\text{O} + 0.53\text{MCO}_3 + 0.53\text{GLYC} + 0.35\text{MGLY} + 0.12\text{MVKN}; k=2.7 \times 10^{-12} \times \exp(350/T)$	$0.965\text{NO}_2 + 0.249\text{HO}_2 + 0.249\text{CH}_2\text{O} + 0.716\text{MCO}_3 + 0.716\text{GLYC} + 0.249\text{MGLY} + 0.035\text{MVKN}; k=2.7 \times 10^{-12} \times \exp(350/T)$
MVK ($\text{VRO}_2 + \text{HO}_2 \rightarrow$)	1.000 VRP; $k=1.82 \times 10^{-13} \times \exp(1300/T)$	$0.38\text{VRP} + 0.62\text{OH} + 0.37\text{GLYC} + 0.37\text{MCO}_3 + 0.13\text{MEK} + 0.25\text{HO}_2 + 0.12\text{MGLY} + 0.12\text{CH}_2\text{O}; k=1.82 \times 10^{-13} \times \exp(1300/T)$
MVK + RCO_3 ($\text{MCO}_3 + \text{HO}_2 \rightarrow$; $\text{RCO}_3 + \text{HO}_2 \rightarrow$; $\text{MAO}_3 + \text{HO}_2 \rightarrow$; $\text{VRO}_2 + \text{HO}_2 \rightarrow$)	$0.16\text{ACTA} + 0.16\text{O}_3 + 0.61\text{OH} + 0.61\text{MO}_2 + 0.23\text{MAP}; k=5.2 \times 10^{-13} \exp(980/T)$ $0.16\text{RCOOH} + 0.16\text{O}_3 + 0.61\text{OH} + 0.61\text{ETO}_2 + 0.23\text{PP}; k=4.3 \times 10^{-13} \exp(1040/T)$ $0.16\text{O}_3 + 0.61\text{OH} + 0.61\text{CO}_2 + 0.61\text{CH}_2\text{O} + 0.21\text{MCO}_3 + 0.40\text{MO}_2 + 0.4\text{CO} + 0.23\text{MAOP}; k=4.3 \times 10^{-13} \exp(1040/T)$ 1.000 VRP; $k=1.82 \times 10^{-13} \times \exp(1300/T)$	$0.16\text{ACTA} + 0.16\text{O}_3 + 0.61\text{OH} + 0.61\text{MO}_2 + 0.23\text{MAP}; k=5.2 \times 10^{-13} \exp(980/T)$ $0.16\text{RCOOH} + 0.16\text{O}_3 + 0.61\text{OH} + 0.61\text{ETO}_2 + 0.23\text{PP}; k=4.3 \times 10^{-13} \exp(1040/T)$ $0.16\text{O}_3 + 0.61\text{OH} + 0.61\text{CO}_2 + 0.61\text{CH}_2\text{O} + 0.21\text{MCO}_3 + 0.40\text{MO}_2 + 0.4\text{CO} + 0.23\text{MAOP}; k=4.3 \times 10^{-13} \exp(1040/T)$ $0.38\text{VRP} + 0.62\text{OH} + 0.37\text{GLYC} + 0.37\text{MCO}_3 + 0.13\text{MEK} + 0.25\text{HO}_2 + 0.12\text{MGLY} + 0.12\text{CH}_2\text{O}; k=1.82 \times 10^{-13} \times \exp(1300/T)$
MACR ($\text{MRO}_2 \rightarrow$)	$1.000\text{CO} + 1.000\text{HAC} + 1.000\text{OH}; k=0$	$1.000\text{CO} + 1.000\text{HAC} + 1.000\text{OH}; k=2.90 \times 10^7 \times \exp(-5297/T)$

Table S3. Revised wavelength bins utilized to define the photolysis frequency of the MVK hydroperoxide in the model.

Lower-bound wavelength (nm)	289	298.25	307.45	312.45	320.30	345	412.45
Upper-bound wavelength (nm)	298.25	307.45	312.45	320.30	345	412.45	850
Base cross section (cm^2)	5.621×10^{-21}	3.573×10^{-21}	2.441×10^{-21}	1.755×10^{-21}	7.405×10^{-22}	4.261×10^{-23}	0
New cross section (cm^2)	5.665×10^{-20}	4.000×10^{-20}	2.740×10^{-20}	2.140×10^{-20}	7.085×10^{-21}	5.634×10^{-22}	0

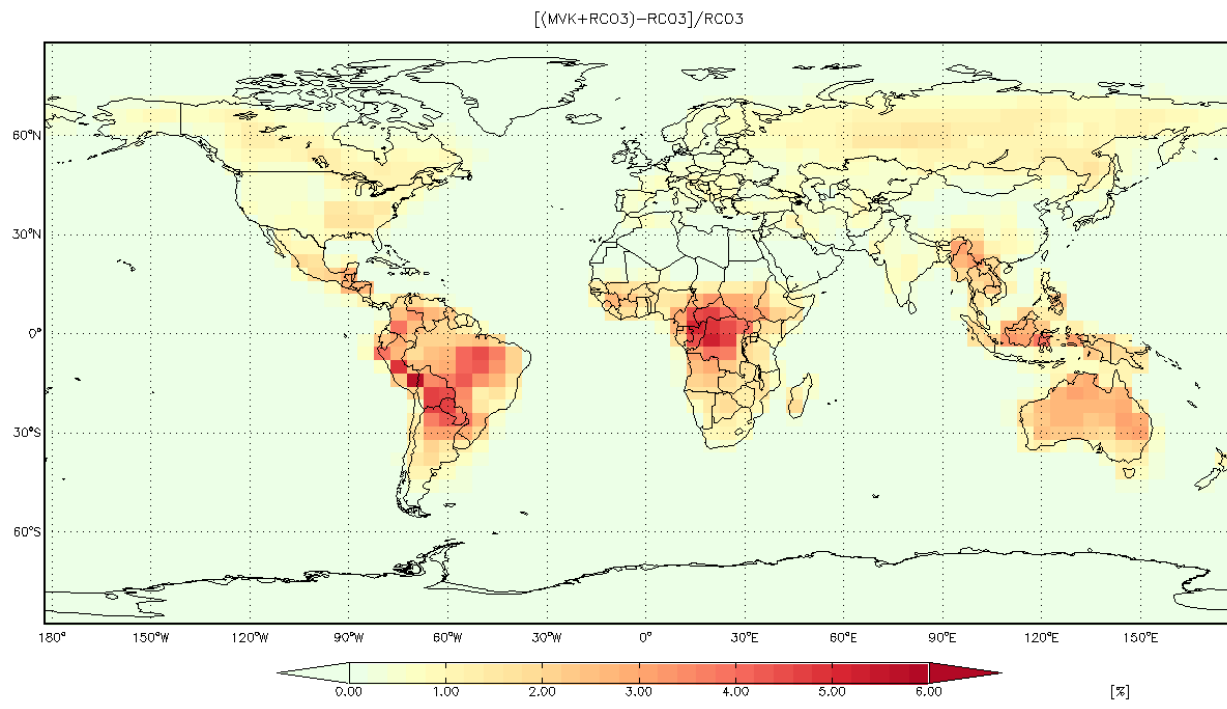


Figure S3. Relative difference in the OH mixing ratio for MVK + RCO₃ in the boundary layer (0-1 km).

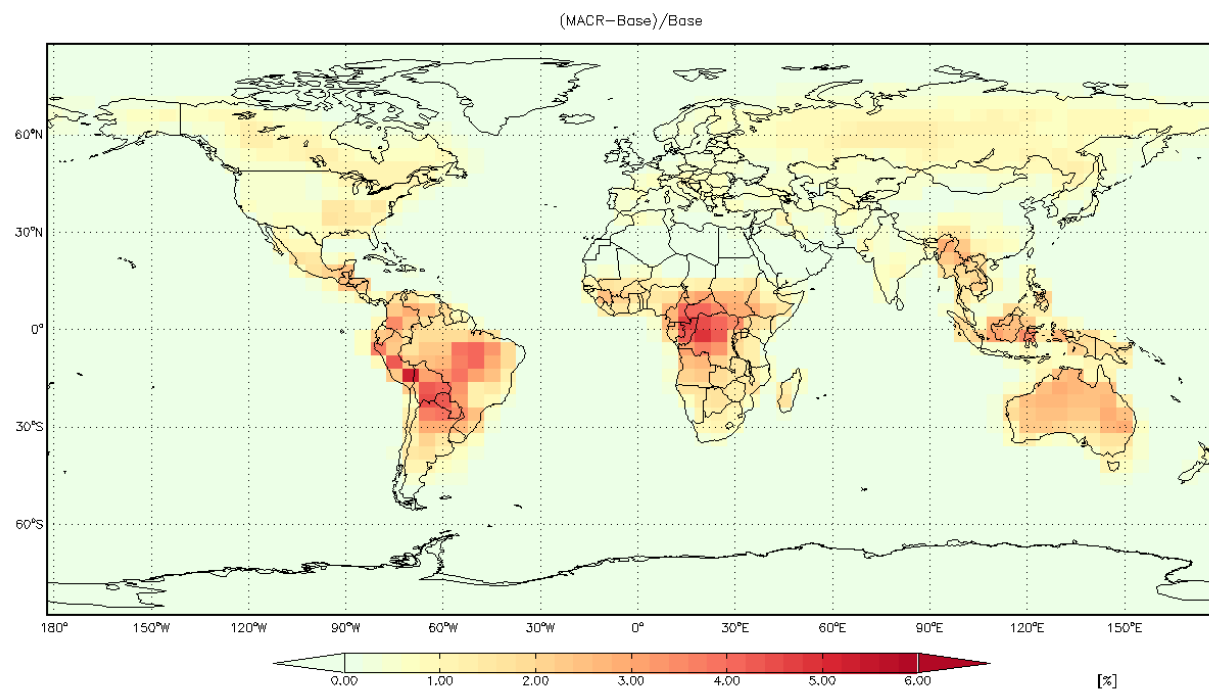


Figure S4. Relative difference in the OH mixing ratio for MACR in the boundary layer (0-1 km).

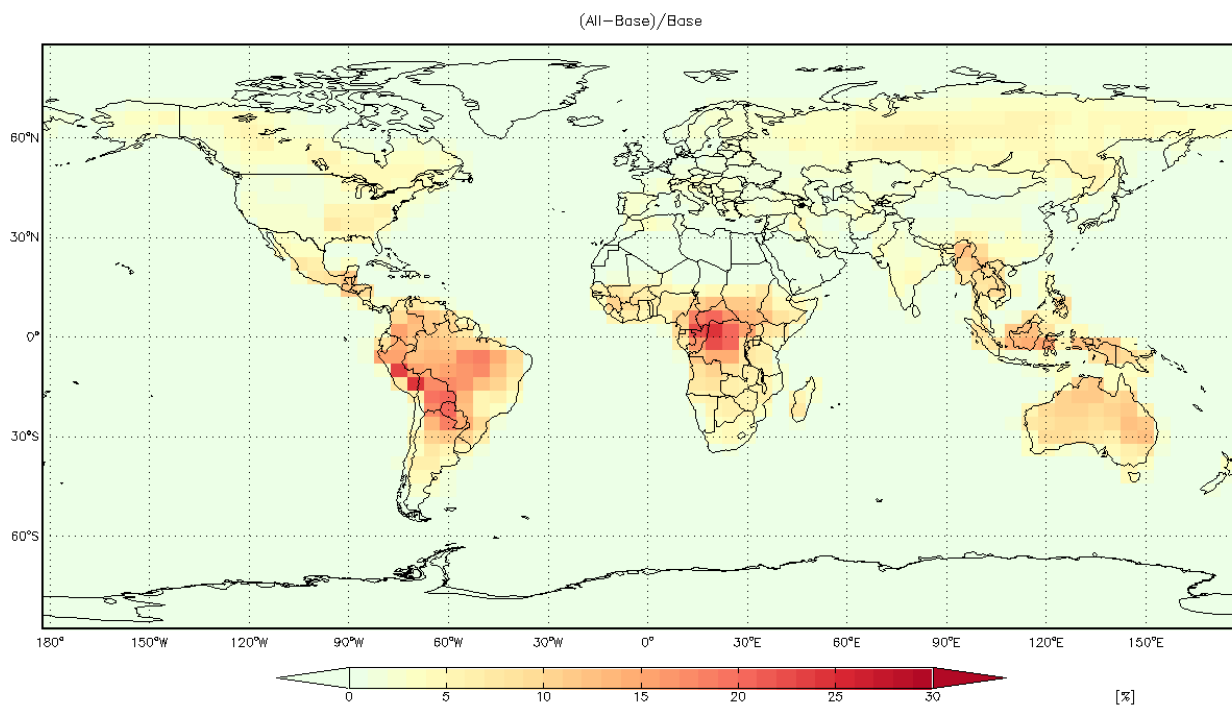


Figure S5. All inclusive: MVK, MACR isomerization, RCO_3 , J_{ROOH} ; relative difference in the boundary layer (0-1 km).

QUANTUM CHEMICAL CALCULATIONS. To test whether using a UHF reference wave function would lower the coupled-cluster energies for the spin-contaminated transition state TS_A , we performed qualitative RHF-RCCSD(T)/6-31+G(d) and UHF-UCCSD(T)/6-31+G(d) single-point energy calculations with the Gaussian 09 program on the wB97xd/aug-cc-pVTZ - optimized geometry. While the UHF energy was 60.5 kcal/mol below the RHF energy, the UHF-UCCSD energy was 344.0 kcal/mol and the UHF-UCCSD(T) energy 272.9 kcal/mol above the RHF-RCCSD and RHF-RCCSD(T) energies, respectively. Inspection of the CCSD iterations (over 300 were required for convergence) indicates that the UCCSD probably converged to the wrong state. A similar comparison for the alternative TS_A isomer, for which CCSD convergence problems did not occur, yielded more modest energy differences, but the UHF-UCCSD(T) energy was still 5.3 kcal/mol above the RHF-RCCSD(T) energy. Spin contamination at the UHF level was extreme for both of the TS_A isomers; $\langle S^2 \rangle = 0.93 \dots 0.95$ before and $0.19 \dots 0.20$ after annihilation. This indicates that using a UHF reference in the coupled cluster calculations would neither lower the barrier, nor improve the reliability of the results and suggests that multireference calculations are required to attain better accuracy. These

problems are likely related to the difficulties of even advanced methods like CCSD(T) or even MRCISD in describing the structure and stability of the HO₃ intermediate product. Varandas et al. has suggested that a quantitative prediction of the dissociation energy of HO₃ would require FCI calculations.⁷

The DFT relative energies for reactant and products are within 4 kcal/mol of the ROHF-ROCCSD(T)-F12/VDZ-F12//wB97XD/aug-cc-pVTZ energies and give an idea of the uncertainty expected in these calculations. For the RI and the TS's the difference is higher than usual and, in conjunction with the spin and T1 values, an indication that multireference calculations are needed to obtain accurate values. The DFT barrier values for the ROOH and R(C=O) channels are such that these products would not be observed. The F12 barriers for these channels are lower and thus in better agreement with experiment.

The formation of intermediate product complexes of energies comparable to that of the reactants allow for back reactions that further complicate determination of yields.

Table S4. Spin contamination and T1 diagnostic in the calculations from the different RO₂ + HO₂ channels

	<S ² > before annihilation ^a	<S ² > after annihilation ^a	T1 ^b
ROO	0.7546	0.7500	0.023
OOH	0.7543	0.7500	0.034
³ TS	2.0124	2.0001	0.032
ROOH	0.0	0.0	0.013
O ₂	2.0101	2.0001	0.008
RI	0.0	0.0	0.016
¹ TS _A	0.5729	0.0167	0.020
RO	0.7577	0.7500	0.028
OH	0.7529	0.7500	0.007
¹ TS _B	0.0	0.0	0.021
R(C=O)	0.0	0.0	0.014

^a In the UwB97XD/aug-cc-pVTZ calculation.

^b In the ROHF-ROCCSD(T)-F12/VDZ-F12//wB97XD/aug-cc-pVTZ calculation.

SECOND TETROXIDE. We have found a second tetroxide that also leads to both RO and R(C=O). It is lower in energy than the one in Figure 4, however the TS leading to the products are higher in energy. These pathways are shown below in Figure S6.

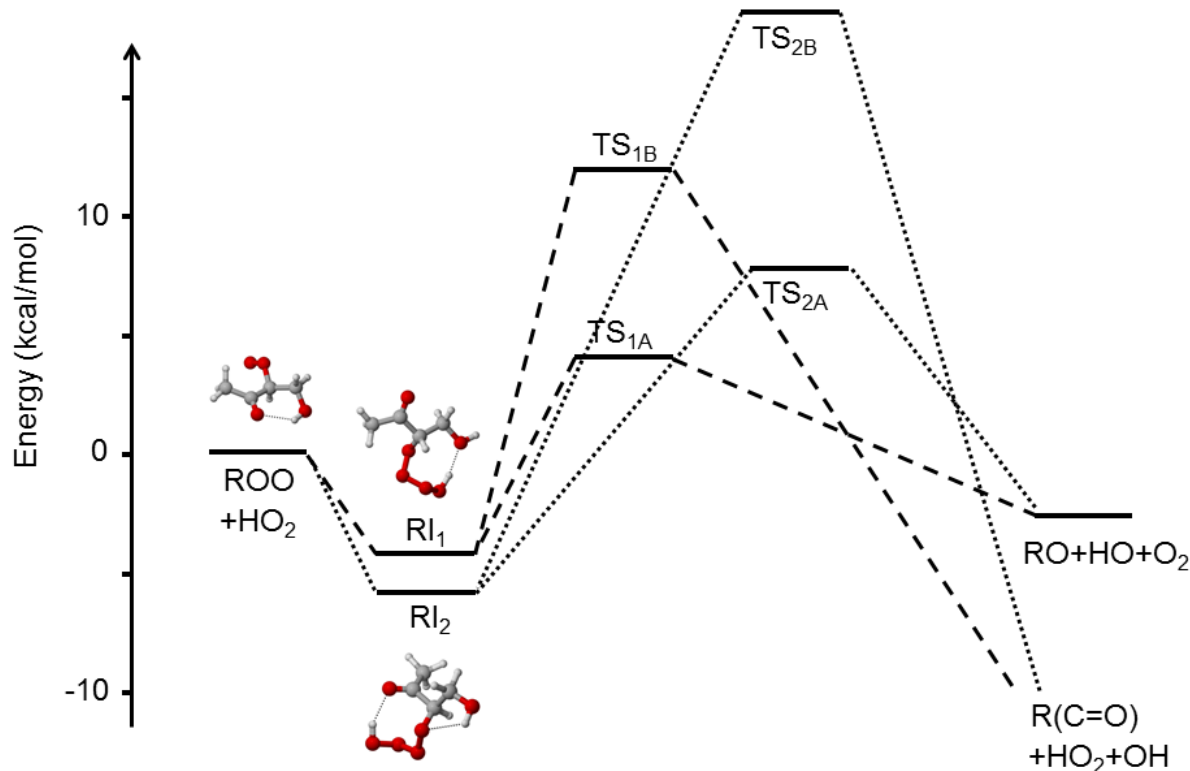


Figure S6. Relative energies (ΔG_{298K}) for the two singlet $RO_2 + HO_2$ channels, including the second tetroxide (RI_2). RI_1 is identical to RI in the manuscript. We have used wB97XD/aug-cc-pVTZ thermochemistry with ROHF-ROCCSD(T)-F12/VDZ-F12 energies. The wB97XD/aug-cc-pVTZ geometries for each of the stationary points are shown.

Table S5. Comparison of the energetics of the channels associated with the two different tetroxides.

	ΔE^a (kcal/mol)	ΔE^b (kcal/mol)	ΔG_{298K}^c (kcal/mol)	TS (imaginary frequency, cm^{-1})
ROO + HO ₂	0.0	0.0	0.0	-
RI≡RI ₁	-12.2	-20.4	-4.1	-
RI ₂	-13.7	-21.7	-6.0	-
TS _{1A} ≡TS _A	+2.5	-8.3	+4.1	212i
TS _{2A}	+3.9	-5.1	+7.8	169i
TS _{1B} ≡TS _B	+11.2	-0.7	+12.0	905i
TS _{2B}	+18.1	+6.7	+18.9	1011i

^a Calculated with wB97XD/aug-cc-pVTZ.

^b Calculated with ROHF-ROCCSD(T)-F12/VDZ-F12//wB97XD/aug-cc-pVTZ.

^c Calculated with the wB97XD/aug-cc-pVTZ thermochemistry with CCSD(T)-F12/VDZ-F12 single point energy correction.

TABLE S6. Spin contamination and T1 diagnostic associated with the second tetroxide RI₂ and its TS.

	<S ² > before annihilation ^a	<S ² > after annihilation ^a	T1 ^b
RI ₂	0.0	0.0	0.016
TS _{2A}	0.6813	0.0250	0.021
TS _{2B}	0.0	0.0	0.022

^a In the UwB97XD/aug-cc-pVTZ calculation.

^b In the ROHF-ROCCSD(T)-F12/VDZ-F12//wB97XD/aug-cc-pVTZ calculated.

DECOMPOSITION OF ALKOXY RADICAL FORMED FROM EXTERNAL OH ADDITION TO MVK (R1a). The decomposition of the alkoxy radical formed in the reaction of NO with the peroxy radical produced in R1a can lead to either methylglyoxal ($\text{CH}_3(\text{C}=\text{O})\text{CHO}$) and the CH_2OH radical or glycolaldehyde (CH_2OHCHO) and the $\text{CH}_3\text{C}=\text{O}$ radical. The calculated energies and stationary points are shown in Figure S7 and Table S7. The barrier of the internal alkoxy decomposition will likely be dominated by glycolaldehyde formation.

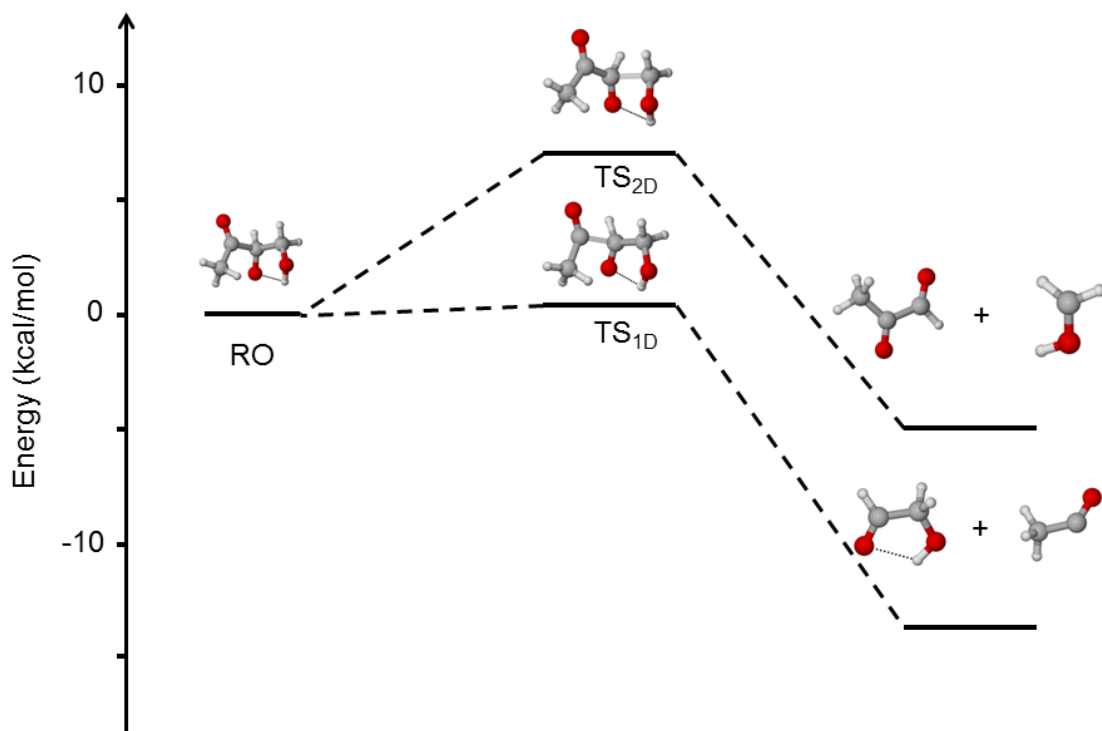


Figure S7. Relative energies ($\Delta G_{298\text{K}}$) for the two decomposition channels of the alkoxy formed from external OH addition to MVK. We have used wB97XD/aug-cc-pVTZ thermochemistry with ROHF-ROCCSD(T)-F12/VDZ-F12 energies. The wB97XD/aug-cc-pVTZ geometries for each of the stationary points are shown.

Table S7. Energetics of the different RO decomposition channels

	ΔE^a (kcal/mol)	ΔE^b (kcal/mol)	ΔG_{298K}^c (kcal/mol)	TS (imaginary frequency, cm^{-1})
RO	0.0	0.0	0.0	-
TS _{1D} ^d	+3.3	+1.5	+0.4	199.4i
Glycolaldehyde+ $\text{CH}_3(\text{C}=\text{O})$	+14.2	+10.5	-5.1	-
TS _{2D}	+9.0	+8.2	+6.9	237.6i
Methylglyoxal+ CH_2OH	+3.9	+0.2	-14.2	-

^a Calculated with wB97XD/aug-cc-pVTZ.

^b Calculated with ROHF-ROCCSD(T)-F12/VDZ-F12//wB97XD/aug-cc-pVTZ.

^c Calculated with the wB97XD/aug-cc-pVTZ thermochemistry with CCSD(T)-F12/VDZ-F12 single point energy correction.

^d Structure optimized and frequencies and thermal contributions to ΔG_{298K} calculated using tight optimization criteria and an ultrafine integration grid in order to remove a spurious near-zero imaginary frequency. For consistency, the DFT energy has been computed with a single-point energy evaluation using the normal integration grid.

Table S8. Spin contamination and T1 diagnostic associated with the second RI and its TS

	$\langle S^2 \rangle$ before annihilation ^a	$\langle S^2 \rangle$ after annihilation ^a	T1 ^b
TS _{1D}	0.7617	0.7500	0.018
CH ₃ (C=O)CHO	0.0	0.0	0.014
CH ₂ OH	0.7534	0.7500	0.020
TS _{2D}	0.7650	0.7501	0.018
CH ₂ OHCHO	0.0	0.0	0.015
CH ₃ (C=O)	0.7542	0.7500	0.016

^a In the UwB97XD/aug-cc-pVTZ calculation.

^b In the ROHF-ROCCSD(T)-F12/VDZ-F12//wB97XD/aug-cc-pVTZ calculation.

Cartesian coordinates for all wB97XD/aug-cc-pVTZ optimized structures, where the electronic energy is in kcal/mol:

:::::::

HO₂

:::::::

3

Energy: -94704.3569035

O	0.05500	0.70969	0.00000
O	0.05500	-0.60177	0.00000
H	-0.87995	-0.86335	0.00000

:::::::

O₂

:::::::

2

Energy: -94336.1957928

O	0.00000	0.00000	0.59799
O	0.00000	0.00000	-0.59799

:::::::

OH

:::::::

2

Energy: -47528.0389744

O	0.00000	0.00000	0.10780
H	0.00000	0.00000	-0.86242

:::::::

R(C=O)

:::::::

13

Energy: -239529.5526856

C	2.30914	-0.66919	-0.04255
C	1.18192	0.31301	0.00906
C	-0.24329	-0.27535	0.01132
C	-1.39271	0.69344	-0.03597
O	-2.62017	0.03653	-0.01120
H	-2.43716	-0.90952	0.01335
O	1.31295	1.50856	0.04493
O	-0.42236	-1.46679	0.04879
H	-1.29524	1.38686	0.80611
H	-1.28369	1.30066	-0.94242
H	2.25549	-1.23220	-0.97580
H	2.20934	-1.39831	0.76132
H	3.25754	-0.14538	0.02616

:::::::

RO

:::::::

14

Energy: -239869.6979721

C	-1.37690	1.22621	-0.42550
C	-1.09636	-0.18405	-0.02779
C	0.29602	-0.43875	0.78587
C	1.34311	-0.75576	-0.32010
H	0.94661	-1.49381	-1.01589
O	-1.76645	-1.13412	-0.26446
O	0.58962	0.64168	1.47266
H	0.07548	-1.33555	1.38137
H	2.20782	-1.19154	0.19185
H	-0.57105	1.56190	-1.07872
H	-1.35224	1.84999	0.46770
H	-2.33661	1.28831	-0.93013
O	1.69503	0.38722	-1.04428
H	1.88927	1.07665	-0.40252

:::::::

ROO

:::::::

15

Energy: -287035.2495299

C	1.55878	1.57985	0.13201
C	0.15972	1.07175	-0.03230
C	-0.05696	-0.43610	-0.19581
O	1.01474	-1.17941	0.41824
O	1.98885	-1.43520	-0.40921
O	-0.80323	1.80041	-0.06267
C	-1.37076	-0.91139	0.42921
O	-2.47270	-0.45315	-0.30298
H	-2.43629	0.50882	-0.29392
H	1.98052	1.20208	1.06463
H	2.19355	1.20020	-0.66966
H	1.55217	2.66538	0.13605
H	-0.05089	-0.66573	-1.26303
H	-1.41653	-0.59664	1.47764
H	-1.38847	-1.99990	0.40264

::::::::::::::::::::

ROOH

::::::::::::::::::::

16

Energy: -287442.6139997

C	-0.46165	1.49173	0.41834
C	-0.13173	0.05885	0.84402
C	1.03478	-0.52184	0.04309
C	2.31811	0.25780	0.05789
O	0.90387	-1.54482	-0.58396
O	-0.54196	1.65401	-0.97611
O	-1.25093	-0.79757	0.83759
O	-1.75897	-0.88717	-0.49368
H	-1.14374	-1.53625	-0.86893
H	-1.19226	1.02115	-1.29412
H	0.32350	2.16328	0.76692
H	-1.39347	1.77623	0.91605
H	0.15907	0.07220	1.89953
H	2.21587	1.07767	-0.65650
H	2.51748	0.69203	1.03731
H	3.14043	-0.38123	-0.25102

::::::::::::::::::::

TS_A

::::::::::::::::::::

18

Energy: -381737.1368787

C	-2.43736	-1.52374	-0.03950
C	-2.02906	-0.09221	-0.22122
O	-2.77994	0.78015	-0.56490
C	-0.53571	0.22410	0.05887
O	-0.06481	-0.56417	1.06244
C	-0.27973	1.71000	0.27226
O	1.11489	1.94334	0.10283
O	1.51014	-1.56530	0.40213
O	1.93182	-1.05700	-0.67108
O	2.92437	-0.04137	-0.41327
H	1.33371	2.82829	0.39104
H	-0.85670	2.29015	-0.44713
H	-0.03848	-0.07099	-0.88719
H	-0.59247	1.97918	1.28347
H	-1.68241	-2.20031	-0.43780
H	-3.40234	-1.68833	-0.50998
H	-2.50755	-1.73311	1.02882
H	2.34558	0.72089	-0.18882

:::::::

TS_B

:::::::

18

Energy: -381728.4030946

C	-2.48856	-1.20372	0.17708
C	-1.83792	0.07721	-0.24390
C	-0.42750	0.33818	0.30742
C	0.17843	1.73039	0.06786
O	1.52551	1.71623	0.50345
H	1.53339	1.31154	1.37837
O	-2.34003	0.91019	-0.95025
O	-0.05572	-0.27530	1.34851
O	1.34345	-1.60812	0.55163
H	0.16922	1.99709	-0.98523
H	0.21883	-0.39537	-0.58218
H	-0.40742	2.47484	0.61343
H	-2.65322	-1.18418	1.25480
H	-1.82264	-2.04571	-0.01576
H	-3.43152	-1.32854	-0.34624
O	1.20018	-1.25371	-0.65559
O	2.28173	-0.35006	-1.13142
H	2.20561	0.40420	-0.49863

:::::::

RI

:::::::

18

Energy: -381751.8518753

C	-2.35127	-1.48241	0.20507
C	-1.98578	-0.06833	-0.13886
C	-0.49290	0.27441	-0.14960
C	-0.21880	1.71319	0.23857
O	1.16077	1.96422	0.00685
H	1.35783	2.87288	0.23143
O	-2.79594	0.77607	-0.42560
O	0.24334	-0.55575	0.74207
O	0.97023	-1.55115	0.04983
H	-0.84911	2.36492	-0.36599
H	-0.12281	0.11361	-1.16495
H	-0.46646	1.86001	1.29365
H	-2.13096	-1.66883	1.25676
H	-1.74213	-2.18197	-0.36838
H	-3.40765	-1.64219	0.01172
O	1.93572	-0.91709	-0.73522
O	2.88274	-0.32752	0.10405
H	2.47893	0.55022	0.23885

::::::::::::::::::

Triplet TS

::::::::::::::::::

18

Energy: -381742.8499081

C	-0.74581	-2.19323	0.87641
C	-1.23424	-1.20273	-0.13674
O	-2.11251	-1.43482	-0.92517
C	-0.59284	0.18718	-0.18587
O	0.44296	0.24849	0.81876
O	1.24612	1.29041	0.63545
C	-1.62526	1.28826	0.05353
O	-1.16962	2.56159	-0.30700
O	2.96015	0.01590	-0.50810
O	2.33312	-1.09095	-0.53149
H	-0.33674	2.73425	0.13822
H	-2.48505	1.06110	-0.57399
H	-0.12388	0.32572	-1.16077
H	-1.94246	1.25012	1.10273
H	-0.86927	-1.78927	1.88249
H	0.32102	-2.36842	0.73760
H	-1.30246	-3.11925	0.77025
H	2.32603	0.70393	-0.00018

::::::::::::::::::

RI₂

::::::::::::::::::

18

Energy: -381753.3123935

C	0.44054	2.45723	-0.76096
C	0.08656	1.29446	0.11912
C	0.73501	-0.04229	-0.24026
C	2.11414	-0.14546	0.41802
O	2.82531	-1.26513	-0.02985
H	2.32702	-2.05166	0.20039
O	-0.64663	1.39942	1.07299
O	0.01066	-1.14363	0.27123
O	-1.01276	-1.52806	-0.62345
H	2.70714	0.73103	0.15898
H	0.84324	-0.14246	-1.32250
H	1.97618	-0.15350	1.50440
H	-0.10259	2.34462	-1.70205
H	1.50320	2.46644	-1.00475
H	0.15025	3.39032	-0.28771
O	-1.95554	-0.50215	-0.68355
O	-2.66617	-0.47099	0.51565
H	-2.10098	0.11597	1.05344

::::::::::::::::::

TS_{2A}

::::::::::::::::::

18

Energy: -381735.6583446

C	0.55967	2.37211	-0.78351
C	0.18419	1.22639	0.11372
C	0.81536	-0.13178	-0.20636
C	2.26894	-0.15347	0.36701
O	2.98943	-1.25373	-0.09400
H	2.53334	-2.05246	0.17852
O	-0.58549	1.36351	1.03489
O	0.20952	-1.19966	0.37865
O	-1.51098	-1.54532	-0.61499
H	2.79185	0.73924	0.02614
H	0.91408	-0.25286	-1.29336
H	2.19791	-0.12471	1.45804
H	-0.17130	2.39905	-1.59528
H	1.54325	2.24902	-1.23367
H	0.49835	3.31062	-0.23930
O	-2.16061	-0.46437	-0.67835
O	-2.83665	-0.20142	0.56271
H	-2.11814	0.26057	1.04245

::::::::::::::::::

TS_{2B}

::::::::::::::::::

18

Energy: -381721.4565748

C	1.39936	-1.15753	-0.68325
C	0.41387	-0.31038	0.12783
C	0.57710	1.22638	0.20328
C	1.83075	1.82552	-0.35632
O	-0.29888	1.88433	0.70962
O	2.60746	-1.34104	0.02057
O	-0.13770	-0.84897	1.12434
H	1.82818	1.71269	-1.44278
H	1.87563	2.88138	-0.10636
H	2.41440	-1.82606	0.82529
H	1.65856	-0.67636	-1.62509
H	0.91378	-2.11223	-0.90393
H	2.70629	1.29489	0.01709
H	-0.69213	-0.31141	-0.68434
O	-1.90813	-0.61401	-0.67848
O	-2.02804	-1.28667	0.38919
O	-2.49366	0.75609	-0.56472
H	-1.95962	1.13539	0.16684

:::::::

TS_{1D}

:::::::

14

Energy: -239866.3562507

O	1.69185	0.27730	-1.14730
C	1.36489	-0.81495	-0.33447
C	0.58811	-0.35300	0.89480
O	0.80484	0.78406	1.33702
H	1.80675	1.02055	-0.54202
H	0.21918	-1.15476	1.55429
H	0.80708	-1.54489	-0.92083
H	2.26665	-1.31793	0.04476
C	-1.29245	-0.19057	-0.01170
O	-1.94284	-1.15853	-0.07919
C	-1.49468	1.21400	-0.44551
H	-1.27259	1.86361	0.39894
H	-0.74857	1.41971	-1.21412
H	-2.50462	1.35816	-0.82401

:::::::

TS_{2D}

:::::::

14

Energy: -239860.6918345

C	1.36190	0.15292	1.33412
C	1.12802	-0.12375	-0.11871
C	0.02281	0.67935	-0.80750
C	-1.48575	-0.82041	-0.43964
O	-1.89654	-0.58299	0.80733
H	-2.23134	0.31857	0.86835
O	1.76327	-0.91305	-0.77433
O	-0.49768	1.66688	-0.28732
H	-2.08698	-0.43575	-1.25560
H	0.00176	0.50741	-1.89753
H	-0.99817	-1.77791	-0.56154
H	0.45808	-0.09059	1.89519
H	1.54125	1.21765	1.48211
H	2.20107	-0.43476	1.69403

:::::::

CH₃(C=O)

:::::::

6

Energy: -96126.6206046

C	0.24589	-0.42765	-0.00002
O	1.25615	0.17232	0.00001
C	-1.16495	0.09765	0.00001

H	-1.67722	-0.29349	-0.87768
H	-1.67724	-0.29373	0.87758
H	-1.18037	1.18867	0.00008

:::::::::::::::::::

Glycolaldehyde

:::::::::::::::::::

8

Energy: -143739.2004389

O	-1.33190	-0.57699	0.00009
C	-0.66700	0.64402	-0.00013
C	0.82590	0.48307	0.00013
O	1.35107	-0.59826	-0.00011
H	-0.65287	-1.26232	0.00028
H	1.41971	1.41434	0.00053
H	-0.93672	1.24348	-0.88003
H	-0.93687	1.24389	0.87943

:::::::::::::::::::

CH₂OH

:::::::::::::::::::

5

Energy: -72208.1163135

C	-0.68029	0.02743	-0.05953
O	0.66649	-0.12522	0.01991
H	1.09619	0.72703	-0.05305
H	-1.11371	0.99497	0.15446
H	-1.23270	-0.88487	0.09649

:::::::::::::::::::

Methylglyoxal

:::::::::::::::::::

9

Energy: -167647.4185019

C	0.87116	1.27366	0.00004
C	0.52316	-0.18109	0.00000
C	-0.96810	-0.54788	0.00014
O	1.31733	-1.08564	-0.00011
O	-1.84394	0.26802	-0.00014
H	-1.15282	-1.63760	0.00058
H	0.42986	1.75545	0.87343
H	0.42896	1.75580	-0.87269
H	1.94955	1.39923	-0.00039

REFERENCES

1. Su, T.; Chesnavich, W. J., Parametrization of the Ion-Polar Molecule Collision Rate-Constant by Trajectory Calculations. *J. Chem. Phys.* **1982**, *76* (10), 5183-5185.

2. Garden, A. L.; Paulot, F.; Crounse, J. D.; Maxwell-Cameron, I. J.; Wennberg, P. O.; Kjaergaard, H. G., Calculation of Conformationally Weighted Dipole Moments Useful in Ion-Molecule Collision Rate Estimates. *Chem. Phys. Lett.* **2009**, 474 (1-3), 45-50.
3. Paulot, F.; Crounse, J. D.; Kjaergaard, H. G.; Kroll, J. H.; Seinfeld, J. H.; Wennberg, P. O., Isoprene Photooxidation: New Insights into the Production of Acids and Organic Nitrates. *Atmos. Chem. Phys.* **2009**, 9 (4), 1479-1501.
4. Teng, A. P.; Crounse, J. D.; Lee, L.; St. Clair, J. M.; Cohen, R. C.; Wennberg, P. O., Hydroxy Nitrate Production in the OH-Initiated Oxidation of Alkenes. *Atmos. Chem. Phys. Discuss.* **2014**, 14 (5), 6721-6757.
5. Lee, L.; Teng, A. P.; Wennberg, P. O.; Crounse, J. D.; Cohen, R. C., On Rates and Mechanisms of OH and O₃ Reactions with Isoprene-Derived Hydroxy Nitrates. *J. Phys. Chem. A* **2014**, 118 (9), 1622-1637.
6. Bey, I.; Jacob, D. J.; Yantosca, R. M.; Logan, J. A.; Field, B. D.; Fiore, A. M.; Li, Q. B.; Liu, H. G. Y.; Mickley, L. J.; Schultz, M. G., Global Modeling of Tropospheric Chemistry with Assimilated Meteorology: Model Description and Evaluation. *J. Geophys. Res.-Atmos.* **2001**, 106 (D19), 23073-23095.
7. Varandas, A. J. C., Ab Initio Treatment of Bond-Breaking Reactions: Accurate Course of HO₃ Dissociation and Revisit to Isomerization. *J. Chem. Theory Comput.* **2012**, 8 (2), 428-441.